CE 566

Uncertainty and Reliability in Civil Engineering

Final Report

Mohammad Moeini

05/09/2021

Optimal Life-Cycle Cost Maintenance Policy for a Deteriorating System Considering Seismic Hazard

Mohammad Moeini

Abstract- In this project, the optimal life-cycle cost analysis for a system of two parallel components under seismic hazard and deterioration is investigated. The project starts from reliability analysis at the component level and adds complexity by exploring the system failure probability under only deterioration effects. Then with a fragility analysis, failure under seismic hazard is characterized for different component states. These past two steps are then used to formulate a Markov Decision Process (MDP) to determine the system's optimal maintenance policy and life-cycle cost. Results indicate that the optimal maintenance policy determined through the MDP formulation yields smaller probabilities of failure than when no maintenance policy is implemented. The results of the MDP are also compared to a Condition Based Maintenance policy.

1 Introduction

This project intends to investigate optimal decision-making actions under uncertainty for a system of two parallel components. To that end, two sources of damage, namely deterioration and seismic hazard, will be considered. The effects of these sources are then combined to formulate the components' overall transition matrices and, subsequently, the system's transition matrices. The consequences of different maintenance actions in determining the are considered through a Markov Decision Process and the optimal life-cycle policy and cost are discovered.

2 Methodology and Results

The effect of component deterioration on the failure probability of each component is quantified through the First Order Reliability Method (FORM). For each component, there are four initial condition states (one to four), and each condition state has a specific limit state function. Therefore there are four different failure probabilities associated with each initial condition state. The results of the FORM analysis are summarized in Table 1.

Table 1. Failure probabilities due to deterioration in different condition states

Condition State	Failure probability
1	0.0003489
2	0.0006989
3	0.0028015
4	0.0069031

Since the sum of each row in the state transition matrix should be equal to unity, the entries of the provided 4×4 transition matrix are scaled to honor this principle. The full 5×5 transition matrix, which now includes the failure probabilities for each component (as condition state five), is therefore as follows:

$$T(s_{t+1}|s_t) = \begin{bmatrix} 0.939672 & 0.059979 & 0 & 0 & 0.000349 \\ 0 & 0.909364 & 0.049965 & 0.039972 & 0.000699 \\ 0 & 0 & 0.817703 & 0.179496 & 0.002802 \\ 0 & 0 & 0 & 0.993097 & 0.006903 \\ 0 & 0 & 0 & 0 & 1.000000 \end{bmatrix} \quad \textbf{(1)}$$

Based on this transition matrix, the annual system probability of failure due to deterioration is calculated in closed form. For this purpose, first, for each component, the annual probability of failure at year n is calculated by multiplying the initial state PMF by T^n. Then considering the parallel configuration of the system, the annual probability of failure is calculated as:

$$\left(P_{f,sys}\right)_i = \left(P_{f,1}\right)_i \times \left(P_{f,2}\right)_i \quad \textbf{(2)}$$

In Eq. **(2)**, $\left(P_{f,sys}\right)_i$ is the annual system failure probability at year i, and $\left(P_{f,1}\right)_i$ and $\left(P_{f,2}\right)_i$ are the annual failure probabilities at year i, for component 1 and 2, respectively. The result of the annual system failure probabilities due to deterioration, with respect to years of service, is depicted in Figure 1.

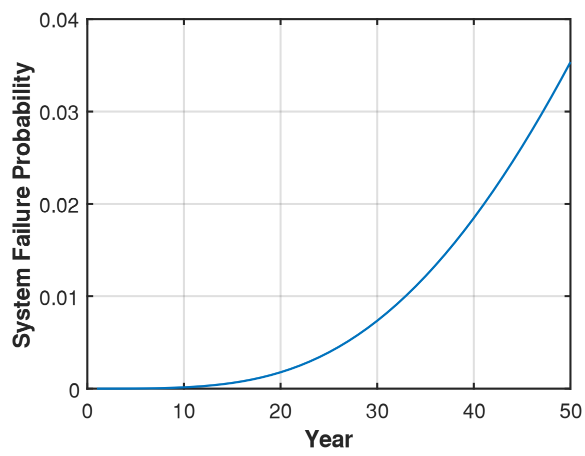

Figure 1. Annual system failure probability under the effect of deterioration

Figure 1 shows that if no maintenance action is implemented, the system failure will constantly increase through the system's service life.

The effect of seismic hazard on the failure of the system is investigated through fragility analysis. To that end, according to provided data, for each of the initial four condition states, based on the methodology explained in (Andriotis and Papakonstantinou 2018), a fragility curve is derived using the data corresponding to each condition state. The resulting fragility curves are shown in Figure 2.

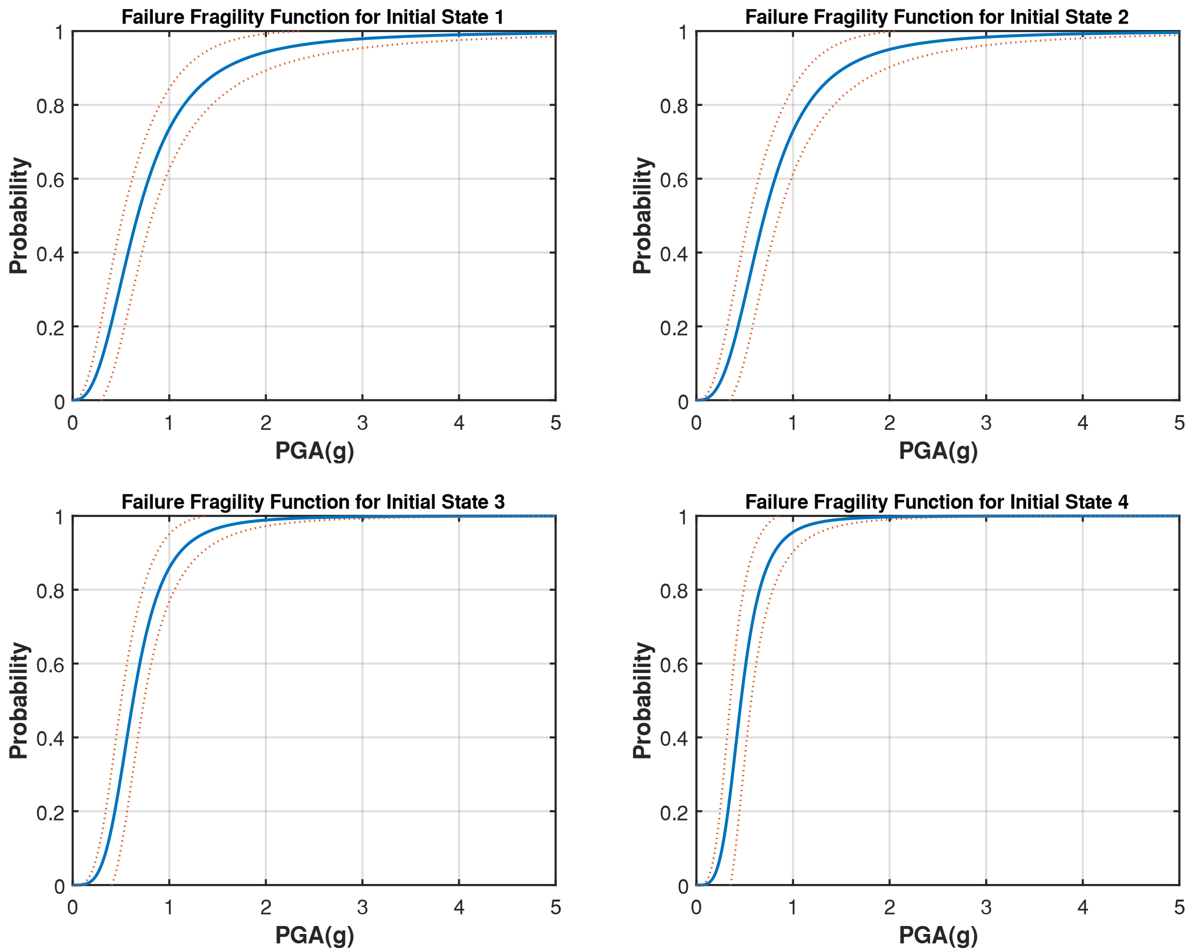

Figure 2. Seismic fragility curves for each initial state

According to Figure 2, it can be observed that for higher condition states, which represent more unsatisfactory system conditions, generally, the probability of failure is higher. Next, to compute the failure probabilities due to the seismic hazard, the Monte Carlo simulation is performed to quantify the expression of Eq. **(3)**.

$$p_f = \lambda_e \int P(DM|IM)\, P(IM|m,r) f_M(m) f_R(r) dmdr \tag{3}$$

In Eq. **(3)**, p_f is the failure probability due to seismic hazard, IM is the intensity measure at each site, which in this project is considered as PGA, and has a Lognormal distribution defined through the attenuation relationship proposed by Campbell and Bozorgnia (2014). $P(DM|IM)$ is the probability of having a certain damage level (here failure due to seismic hazard), which is provided by the fragilities of each state. The magnitude (m) and the distance (r) are treated as deterministic values. Finally, λ_e is the annual probability of earthquake occurrence, which is equal to 0.02. In this project, a scenario-based simulation with 10^6 samples is performed to quantify p_f. The updated transition matrix for each component due to deterioration or earthquake is therefore formed as:

$$T_1(s_{t+1}|s_t) = \begin{bmatrix} 0.93937 & 0.059960 & 0 & 0 & 0.000675 \\ 0 & 0.909104 & 0.049951 & 0.039961 & 0.000984 \\ 0 & 0 & 0.817453 & 0.179441 & 0.003106 \\ 0 & 0 & 0 & 0.992613 & 0.007387 \\ 0 & 0 & 0 & 0 & 1.000000 \end{bmatrix} \tag{4}$$

$$T_2(s_{t+1}|s_t) = \begin{bmatrix} 0.938649 & 0.059914 & 0 & 0 & 0.001437 \\ 0 & 0.908408 & 0.049913 & 0.039930 & 0.001749 \\ 0 & 0 & 0.816738 & 0.179284 & 0.003978 \\ 0 & 0 & 0 & 0.991588 & 0.008412 \\ 0 & 0 & 0 & 0 & 1.000000 \end{bmatrix} \tag{5}$$

From Eqs. (4) and (5), it can be deduced that the failure probability for component 2 is higher than that of component 1, which is expected since component 2 is closer to the fault; therefore, the seismic energy is less attenuated compared to component 1. Figure 3 compares the effects of deterioration and seismic hazard on the annual system failure probability to when only one source of failure was present (i.e., deterioration).

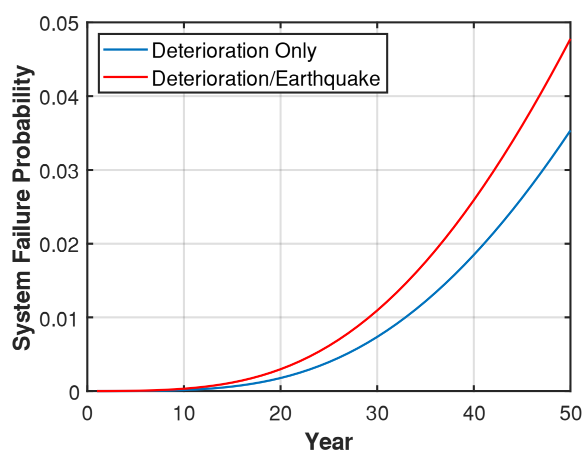

Figure 3. Comparison of the effect of the presence of only deterioration to the presence of both the deterioration and earthquake

Having the final transition matrices for each component, system MDP can be formulated for this configuration. Since each component has five condition states, the total number of system states will be 25. Two maintenance actions are considered for each component, namely repair or no repair; therefore, the total number of actions for the system will be four (no repair, repair 1 and do not repair 2, repair 2 and do not repair 1, and repair both). Knowing that the repair actions will perfectly restore the system to state 1, the transition matrices for each of the four actions are formulated based on the corresponding component transition matrices. The transition matrices for each action are visualized through heatmaps in Figure 4.

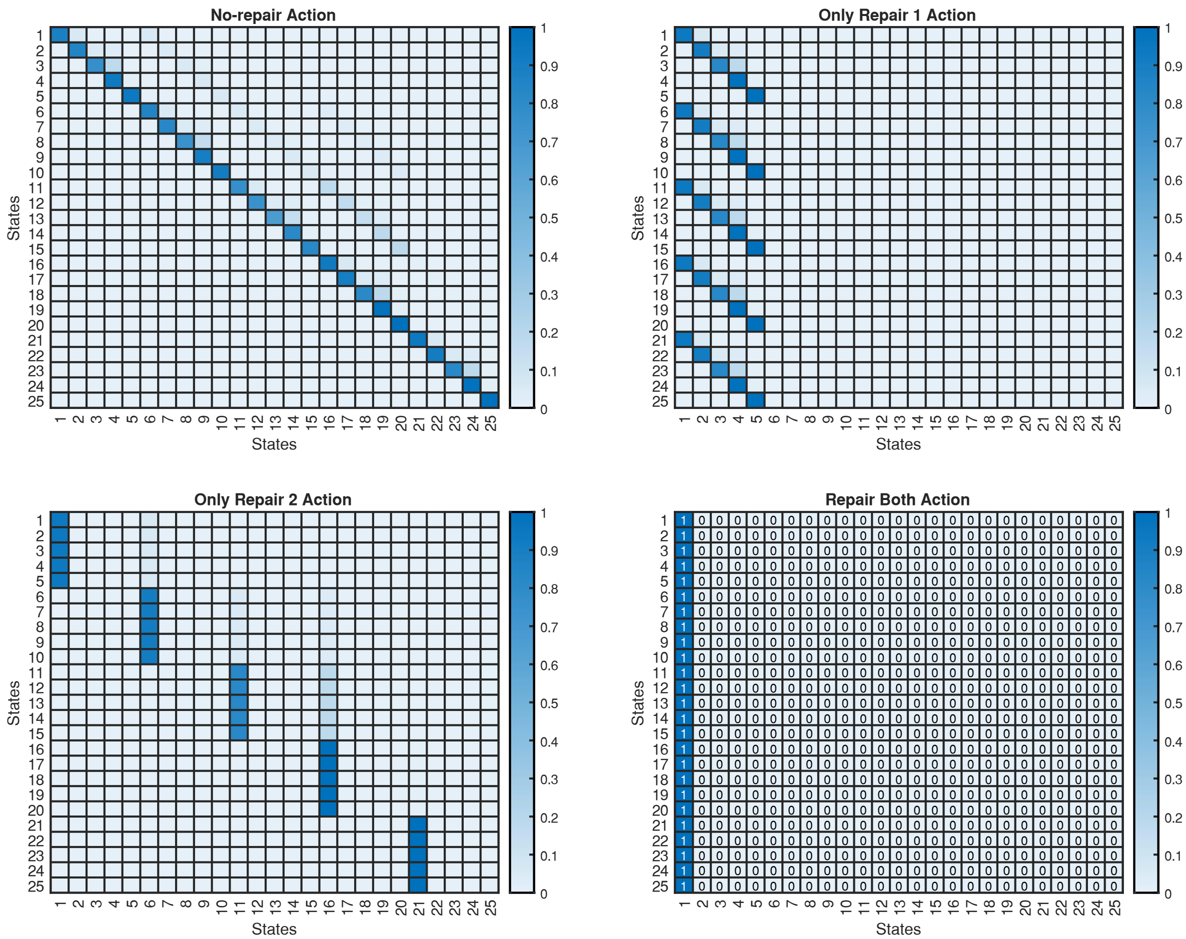

Figure 4. Heatmap visualization of the transition matrices of the four actions

The optimum policy is determined through dynamic programming (Bellman 1952) by choosing the action with the least cost given the state. The appropriate action in each year and state is then selected as the maintenance policy. The heat map visualization of the overall optimum policy and value function is presented in Figure 5.

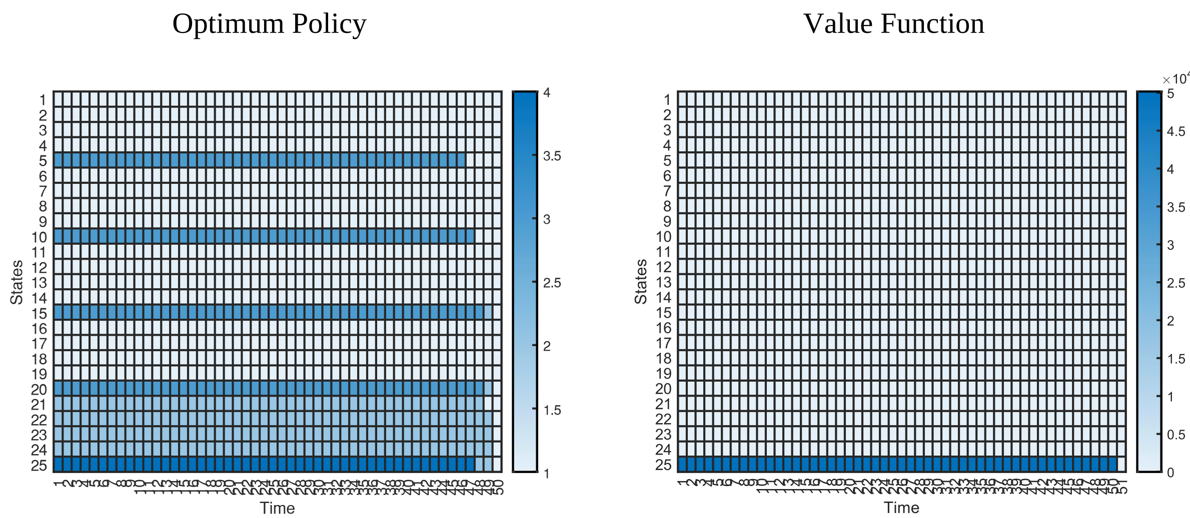

Figure 5. Heatmap visualization of the overall optimum policy and the value function

A Monte Carlo simulation is also performed to show a realization of the system state during the system's lifespan, starting from its initial state. For this purpose, each year, the system state is updated through random sampling with the weights given by the appropriate transition probabilities corresponding to the action taken at the previous year.

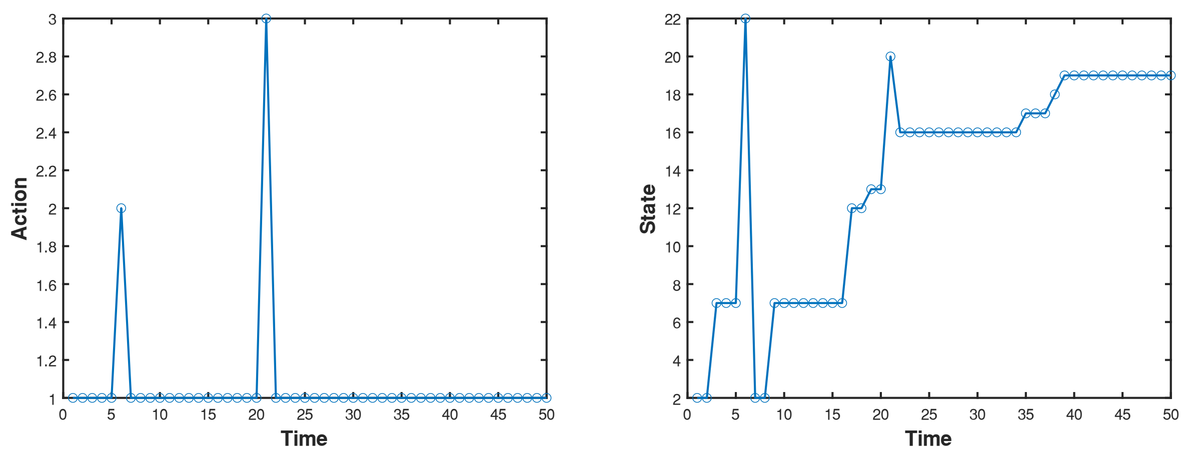

Figure 6. One realization of the system state during its lifespan

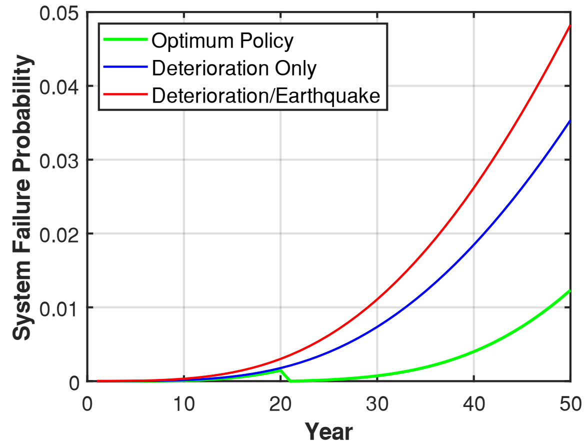

Figure 7. Comparison of the system failure probability when optimum policy adopted with 'no repair' policies

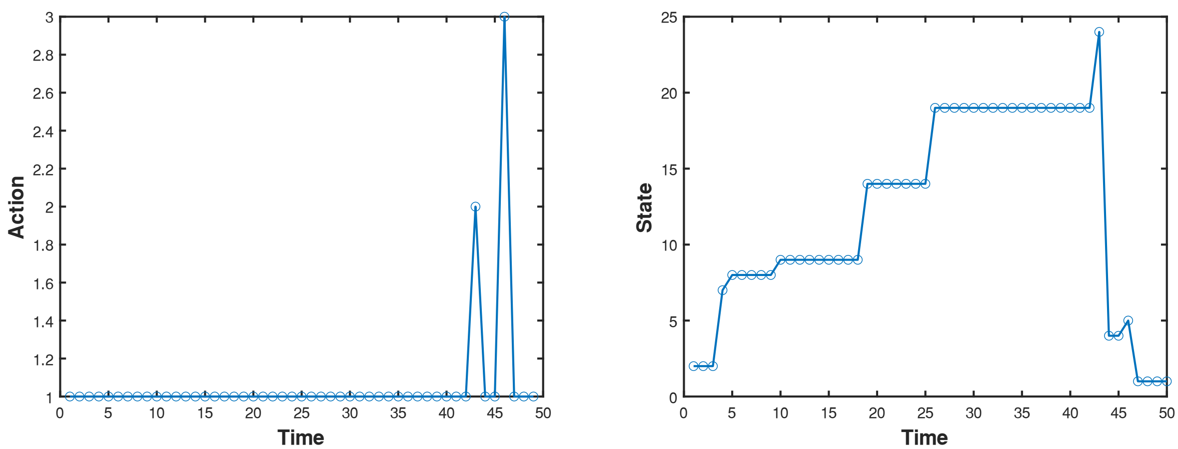

Figure 8. One realization of the system state during its lifespan

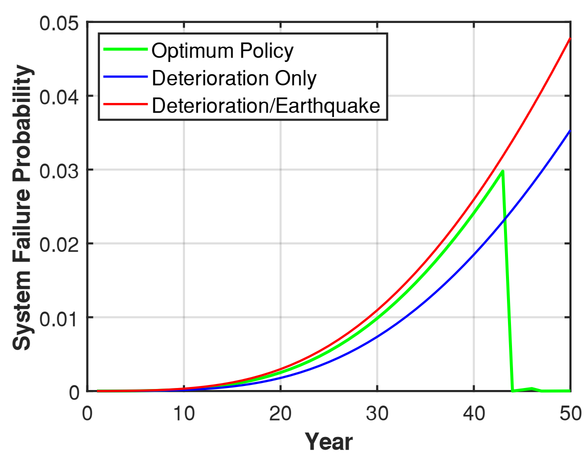

Figure 9. Comparison of the system failure probability when optimum policy adopted with 'no repair' policies

The results shown in Figure 6 to Figure 9 show that the drops in the system failure probability coincide with the maintenance actions, meaning that the maintenance has reduced the failure probability. For the latter realization, the cumulative cost of the optimum policy is also depicted in Figure 10, where it can be observed that with each maintenance action, the cost increases, but in the following years, the cost of the system will be close to none.

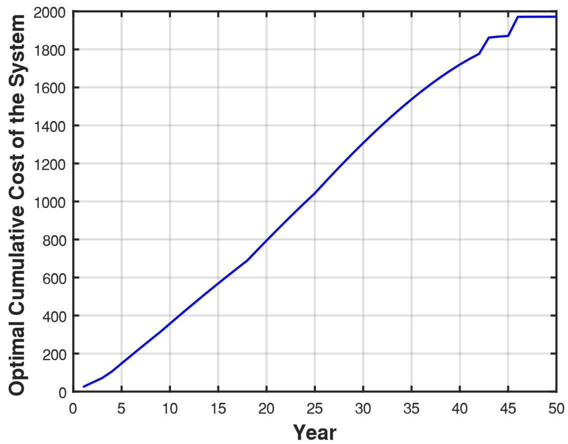

Figure 10. The cumulative cost of the system maintenance during its lifetime when the optimal policy is adopted

Finally, the results of the MDP are compared to a Condition Based Maintenance policy in which the policy is to repair the system whenever each component reaches state 3 or above. The actions in this maintenance policy are either ‘no repair’ or repair both (i.e., a total of two actions). For this purpose, the dynamic programming formulation is updated to select a policy that reflects the appropriate action when the system state matches the corresponding component states that require repair action.

The results are also presented in the form of the overall optimum policy and value function as well as a realization and its optimal cumulative cost in Figure 11 to Figure 14. According to the comparison of failure probabilities in Figure 13, the CBM policy will have a smaller failure probability since its action is taken earlier and has the repair effect on both of the components, however since no action is taken after that, the failure probability at the last year of the service is above that of the optimum policy determined through MDP formulation. According to Figure 14, it is also observed that since in CBM repair action is implemented earlier, the final cost of the system is higher than that of the optimum policy, meaning that the optimum policy has both a lower total cost and a lower final probability of failure (at the last year of the service).

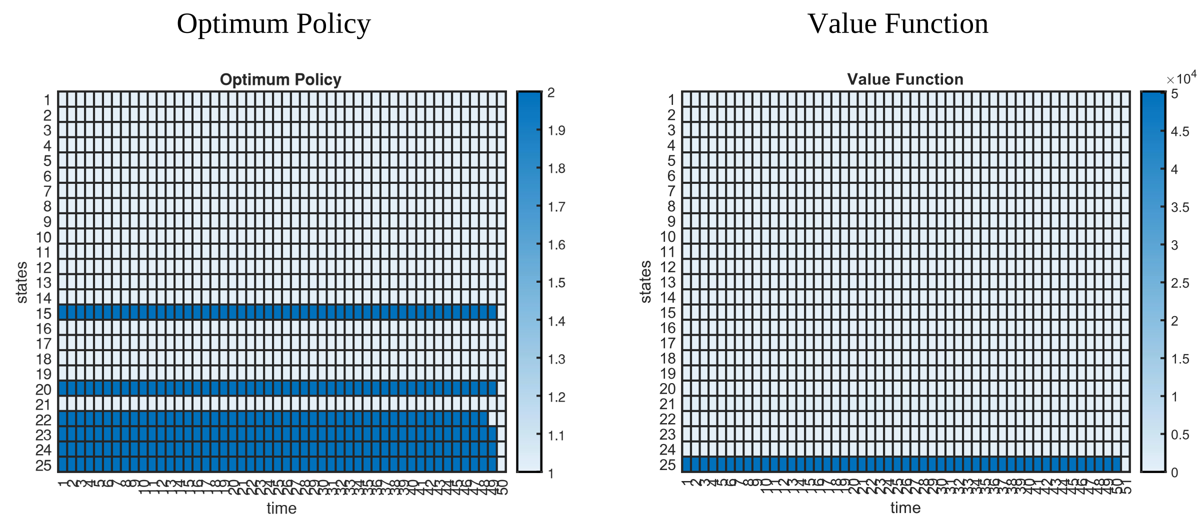

Figure 11. Heatmap visualization of the overall optimum policy and the value function for CBM

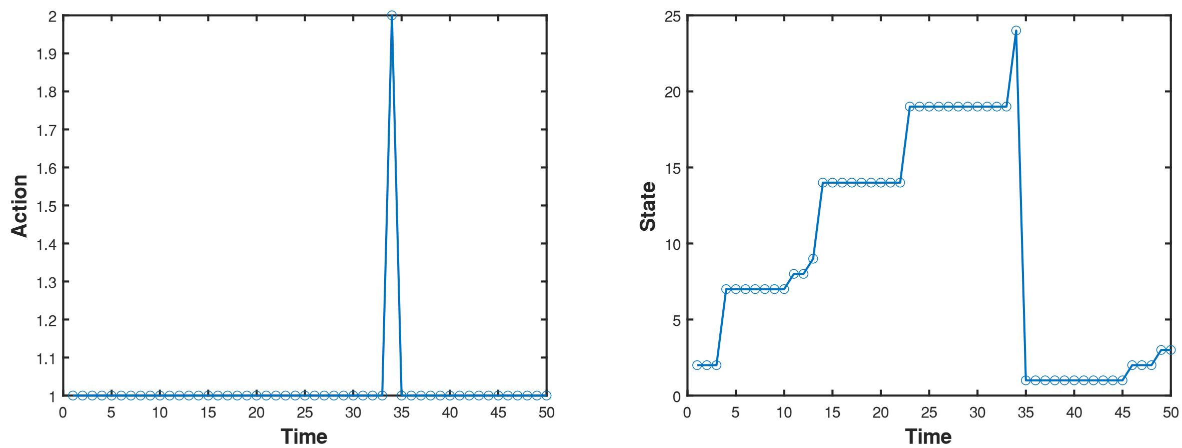

Figure 12. One realization of the system state during its lifespan for CBM

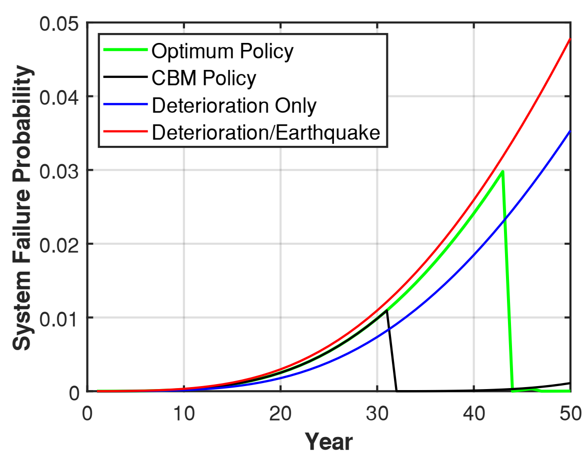

Figure 13. Comparison of the system failure probability when optimum policy adopted with 'no repair' policies-CBM and MDP compared

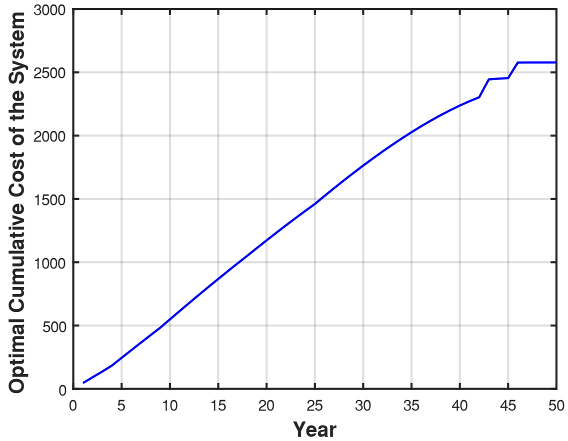

Figure 14. The cumulative cost of the system maintenance during its lifetime when the optimal policy is adopted-CBM

3 Conclusions

In this project, the optimal life-cycle cost analysis of a deteriorating system under seismic hazard was performed. Failure probabilities due to deterioration and seismic hazard were quantified by FORM and fragility analysis, respectively. The system Markov Decision Process (MDP) was formulated to determine the system's optimal maintenance policy and life-cycle cost. Results indicate that the optimal maintenance policy determined through the MDP formulation yields smaller probabilities of failure than when no maintenance policy is implemented. The results of the MDP are also compared to a Condition Based Maintenance policy.

4 References

Andriotis, C. P., and Papakonstantinou, K. G. (2018). “Extended and generalized fragility functions.” *Journal of Engineering Mechanics*, American Society of Civil Engineers, 144(9), 4018087.

Bellman, R. (1952). “On the theory of dynamic programming.” *Proceedings of the National Academy of Sciences of the United States of America*, National Academy of Sciences, 38(8), 716.

Campbell, K. W., and Bozorgnia, Y. (2014). “NGA-West2 ground motion model for the average horizontal components of PGA, PGV, and 5% damped linear acceleration response spectra.” *Earthquake Spectra*, SAGE Publications Sage UK: London, England, 30(3), 1087–1115.